INT. J. NUM. METH. HEAT FLUID FLOW, VOL. 5, 531–547 (1995)

A COUPLED MODEL FOR WATER FLOW, AIRFLOW AND HEAT FLOW IN DEFORMABLE POROUS MEDIA

BERNARD A. SCHREFLER, XIAOYONG ZHAN AND LUCIANO SIMONI

Istituto di Scienza e Tecnica delle Costruzioni, University of Padova, Padova, Italy

ABSTRACT

A fully coupled numerical model to simulate the complex behaviour of soil deformation, water flow, airflow, and heat flow in porous media is developed. The following thermal effects are taken into account: heat transfer through conduction and convection, flow, as well as viscosity and density variation of the fluids due to temperature gradients. The governing equations in terms of soil displacements, water and air pressures, and temperature are coupled non-linear partial differential equations and are solved by the finite element method. Two examples are presented to demonstrate the model performances.

KEY WORDS Soil deformation Finite element Porous media Heat transfer

NOMENCLATURE

Subscripts or superscripts

a	air
w	water
s	soil
π	air, water,or soil
h	horizontal
v	vertical

Other symbols

q	flux
atm	atmospheric condition
ref	reference condition
o	initial conditions
	(overbar) boundary conditions
Γ	boundary
n_i	normal vector at boundary
p	pressure
p_c	capillary pressure
S	saturation
w_i	velocity
k	permeability
k_i	absolute permeability
k_r	relative permeability
μ	dynamic viscosity
ρ	density
T	temperature
λ_{ij}	thermal conductivity
Q	heat source or sink
β	thermal expansion coefficient
C	heat capacity
n	porosity
K	bulk modulus
u_i	displacement
ε_{ij}	strain
$d\varepsilon_{ij}^T$	strain caused by thermoelastic expansion
$d\varepsilon_{ij}^p$	plastic strain increment
σ_{ij}	total stress
σ''_{ij}	modified effective stress
α	Biot's constant
D_{ijkl}	tangent matrix
b_i	body force

INTRODUCTION

A fully coupled model to simulate isothermal water flow and airflow in deforming porous media has recently been proposed by Schrefler and Zhan[1]. This model is now extended to also take

0961–5539/95/060531–17$2.00

Received November 1993
Revised January 1994

into account nonisothermal conditions. A proper model for heat and mass transfer in partially saturated porous media should consider in addition to the linear momentum balance equation for the whole mixture (equilibrium equation), an energy balance equation taking into account latent heat transfer and at least two mass conservation equations. These last two equations result from the sum of the mass conservation equations of the separate phases considered in the simulation. More traditional methods used complex transfer coefficients[2]. A numerical solution of a full model of the first type described above does not yet exist to our knowledge and the model presented in this paper is only a step towards this goal.

Only few published solutions can be found for heat and mass transfer in unsaturated deforming porous media. This appears clearly from the extensive survey by Alonso *et al.*[3] on the general topic of partially saturated porous media. The following publications are chosen to point out the different approaches present in the literature.

A one-dimensional heat and moisture transfer model in a rigid unsaturated soil was presented by Dakshanamurthy and Fredlund[4]. The model considers liquid flow (no vapour flow), gas flow and heat flow equation, which is uncoupled from the other two conservation equations. The liquid flow equation neglects flow due to temperature gradient and the heat flow equation considers only flow due to conduction. The permeability is constant as well as the density of the mixture. Thomas[5] used one moisture continuity equation which describes both liquid and vapour flow. De Vries' theory with modifications along the lines of Luikov's work[6] is used in the heat conservation equation. No solid deformation is considered. The variables are temperature and volumetric moisture content. Capillary potential and temperature were used in a more recent paper by Thomas and King[7] for heat and mass transfer analysis in rigid unsaturated soil. Baggio *et al.*[8] presented a model for rigid matrix with three conservation equations: one for energy, one for dry air, and one for water phase (liquid and vapour). In the energy balance equation latent heat transfer and convection are accounted for. Geraminegad and Saxena[9] put forward a thermoelastic model for heat and mass transfer in partially saturated soil. A modified version of Philip and de Vries' formulation is applied in the heat transfer equation. Two mass transfer equations are used and the variables of the model are temperature, capillary and gas pressure. The model incorporates only volumetric soil deformation and neglects hence soil deformation due to external loading. A model for heat and mass transfer in deforming geothermal reservoirs was presented by Lewis *et al.*[10]. In that instance capillary pressure effects can be neglected so that a unique continuity equation for both steam and water was used.

From this short survey it follows that there is ample space for a model for unsaturated nonisothermal flow in deforming porous media such as that one presented in the following. Demand for such a model also results from the design of nuclear waste disposal sites in clay or salt deposits, where not always fully saturated situations prevail and mechanical aspects become important.

Our model solves by means of the finite element method the linear momentum balance equation for the whole mixture, the mass balance equations for solid, air and water and the energy balance equation again for the mixture. It makes use of the modified effective stress concept together with the capillary pressure relationship. In the presented formulation, the mass balance equation for the solid is summed with the mass balance equations of the fluids[11]. The primary variables are displacements of the solid skeleton, water pressure, air pressure and temperature. At this stage the model neglects latent heat transfer, but considers heat transfer through conduction and convection and flow both due to pressure gradient and to temperature gradient. The limits of its applicability are indicated in the next section, where the physical model is presented in more detail. Two examples reported at the end of the paper demonstrate that the model and its solution procedure are reasonable and applicable. The first example is used for validation of the model and comparisons are made with the results of a fully saturated simulator[12] for several sets of parameters. Partially saturated conditions are then analysed. The second example, previously analysed in Reference 4, shows the potential of the model in a case of thermal transport, simulating in a simplified way, evaporation and infiltration at a boundary surface.

THE PHYSICAL MODEL

The physical model is the same as that in Reference 1. Here and in the following sections only the modifications due to the introduction of non-isothermal conditions are shown.The capillary pressure, relating water pressure p_w and air pressure p_a, is now a function of the water saturation S_w and temperature T

$$p_c = p_c(S_w, T) \tag{1}$$

Relation (1) is experimentally determined and usually shows hysteresis, which, at present, is disregarded. Equation (1) is numerically inverted to obtain,

$$S_w = S_w(p_c, T) \tag{2}$$

For the constitutive law of the solid phase a modified effective stress tensor σ''_{ij} is used, as defined in Reference 11:

$$\sigma''_{ij} = \sigma_{ij} + \alpha\delta_{ij}p \tag{3}$$

where σ_{ij} is the total stress tensor, α is the Biot's constant and

$$p = S_a p_a + S_w p_w \tag{4}$$

represent a fluid averaged pressure.

The constitutive relationship for the solid skeleton is now,

$$\mathrm{d}\sigma''_{ij} = D_{ijkl}(\mathrm{d}\varepsilon_{kl} - \mathrm{d}\varepsilon^T_{kl} - \mathrm{d}\varepsilon^p_{kl}) \tag{5}$$

where $\mathrm{d}\varepsilon^T_{kl} = \delta_{kl}\dfrac{\beta_s}{3}\mathrm{d}T$, is the strain caused by thermoelastic expansion; $\mathrm{d}\varepsilon^p_{kl}$ the plastic strain increment and D_{ijkl} is a temperature dependent tangent matrix. Thermal equilibrium is assumed between soil, air and water. This implies that the temperature is the same for the three constituents. The temperature is assumed to be always far below the critical temperature of water. This excludes the modelling of geothermal reservoirs with high temperatures. Furthermore phase change phenomena (evapo-transpiration) must be negligible. Our model allows to evaluate the influence of visocosity and density variation due to temperature gradients. As a first approach all the heat transfer phenomena are taken into account in the experimentally derived constitutive equation for the effective thermal conductivity tensor $\lambda_{ij}(S_w, T)$ and in convection effects. The model applies furthermore only to geomaterials where the main mass transport mechanism for the aqueous phase is flow of liquid water. Investigations are at present made to eliminate all these limitations.

GOVERNING EQUATIONS

We consider only slow phenomena and small displacements. For a full account of the theory, using more complex arguments which confirm the equations derived below, the interested reader is referred to References 11, 13 or 14.

The linear momentum balance equation for the whole mixture, in terms of total stresses reads as,

$$\sigma_{ki,k} + \rho b_i = 0 \tag{6}$$

where ρ is the mixture mass density and b_i is the specific body force.

The linear momentum balance equation for each fluid phase yields Darcy's law[15],

$$w^\pi_i = k_\pi(-p_{\pi,i} + \rho_\pi b^\pi_i) \qquad \pi = w, a \tag{7}$$

where the permeability of the medium to the π fluid,

$$k_\pi = \frac{k_i}{\mu_\pi} k_{r\pi} \tag{8}$$

is now temperature dependent, mainly because of dynamic viscosity $\mu_\pi = \mu_\pi(T)$.

The mass balance equations for the fluid phases[1],

$$\rho_\pi S_\pi \frac{\alpha - n}{K_s} \dot{p} + \alpha \rho_\pi S_\pi \dot{\varepsilon}_{ii} + n \rho_\pi \dot{S}_\pi + (\rho_\pi w_i^\pi)_{,i} + S_\pi n \dot{\rho}_\pi = 0 \tag{9}$$

is now transformed to account for the densities dependence on pressure and temperature. Equation (9) also allows to take into account flow due to temperature gradient. Fron the equation of state for the fluid phases, we have[12],

$$\frac{\dot{\rho}_\pi}{\rho_\pi} = \frac{\dot{p}_\pi}{K_\pi} - \beta_\pi \dot{T} \tag{10}$$

The solid density rate $\frac{\dot{\rho}_s}{\rho_s}$ which is contained in the first term of (9) and is expressed in isothermal condition as $\dot{p}/K_s$, becomes now,

$$\frac{\dot{\rho}_s}{\rho_s} = \frac{\dot{p}}{K_s} - \beta_s \dot{T} \tag{11}$$

Because of the temperature dependence of S_w through equation (2), we have,

$$\dot{S}_w = \frac{\partial S_w}{\partial p_c} \dot{p}_c + \frac{\partial S_w}{\partial T} \dot{T} \tag{12}$$

and hence

$$\dot{p} = \left[S_w + (p_a - p_w) \frac{\partial S_w}{\partial p_c} \right] \dot{p}_w + \left[S_a - (p_a - p_w) \frac{\partial S_w}{\partial p_c} \right] \dot{p}_a - (p_a - p_w) \frac{\partial S_w}{\partial T} \dot{T} \tag{13}$$

The mass balance equation for water and air, after introduction of Darcy's law and equations (10), (11) and (13), are then written, respectively, as,

$$\left[\frac{\rho_w S_w^2 (\alpha - n)}{K_s} + \frac{\rho_w S_w n}{K_w} \right] \dot{p}_w + \frac{\rho_w S_w S_a (\alpha - n)}{K_s} \dot{p}_a + \left[-\frac{S_w (\alpha - n)}{K_s} \rho_w p_c \frac{\partial S_w}{\partial p_c} + n \rho_w \frac{\partial S_w}{\partial p_c} \right] (\dot{p}_a - \dot{p}_w)$$
$$+ \left[-\frac{S_w (\alpha - n)}{K_s} \rho_w p_c \frac{\partial S_w}{\partial T} + n \rho_w \frac{\partial S_w}{\partial T} - [n \beta_w + (\alpha - n) \beta_s] \rho_w S_w \right] \dot{T} + \alpha \rho_w S_w \dot{u}_{i,i} + [\rho_w k_w (-p_{w,i} + \rho_w b_i^w)]_{,i} = 0 \tag{14}$$

$$\left[\frac{\rho_a S_a^2 (\alpha - n)}{K_s} + \frac{\rho_a S_a n}{K_a} \right] \dot{p}_a + \frac{\rho_a S_w S_a (\alpha - n)}{K_s} \dot{p}_w - \left[\frac{S_a (\alpha - n)}{K_s} \rho_a p_c \frac{\partial S_w}{\partial p_c} + n \rho_a \frac{\partial S_w}{\partial p_c} \right] (\dot{p}_a - \dot{p}_w)$$
$$+ \left[\frac{S_a (\alpha - n)}{K_s} \rho_a p_c \frac{\partial S_w}{\partial T} + n \rho_a \frac{\partial S_w}{\partial T} - [n \beta_a + (\alpha - n) \beta_s] \rho_a S_a \right] \dot{T} + \alpha \rho_a S_a \dot{u}_{i,i} + [\rho_a k_a (-p_{a,i} + \rho_a b_i^a)]_{,i} = 0 \tag{15}$$

In the nonisothermal case an energy balance equation is necessary for the whole mixture. By neglecting mechanical heat generation, this balance equation may be written as[16],

$$\overline{\rho C} \dot{T} + S_w \rho_w C_w w_i^w T_{,i} + S_a \rho_a C_a w_i^a T_{,i} = (\lambda_{ij} T_{,j})_{,i} + Q \tag{16}$$

where $\rho C=(1-n)\rho_s C_s+nS_w\rho_w C_w+nS_a\rho_a C_a$ is the heat capacity, $Q=(1-n)\rho_s Q_s+nS_w\rho_w Q_w+nS_a\rho_a Q_a$ the source term of the mixture (the sum of the terms Q_π of each constituent). The second and the third terms are the heat transfer through convection. After introduction of equations (10)-(13) and of Darcy's law, the energy balance equation becomes,

$$\left[\frac{(1-n)\rho_s C_s}{K_s}\left(S_w+p_c\frac{\partial S_w}{\partial p_c}\right)-n\rho_w C_w\frac{\partial S_w}{\partial p_c}+\frac{nS_w\rho_w C_w}{K_w}+n\rho_a C_a\frac{\partial S_w}{\partial p_c}\right]T\dot{p}_w$$
$$+\left[\frac{(1-n)\rho_s C_s}{K_s}\left(S_a-p_c\frac{\partial S_w}{\partial p_c}\right)+n\rho_w C_w\frac{\partial S_w}{\partial p_c}+\frac{n(1-S_w)\rho_a C_a}{K_a}-n\rho_a C_a\frac{\partial S_w}{\partial p_c}\right]T\dot{p}_a$$
$$\left\{\left[\frac{(n-1)\rho_s C_s}{K_s}p_c\frac{\partial S_w}{\partial T}+(n-1)\beta_s\rho_s C_s+n\rho_w C_w\frac{\partial S_w}{\partial T}-nS_w\beta_w\rho_w C_w\right.\right.$$
$$\left.\left.-n\rho_a C_a\frac{\partial S_w}{\partial T}-n(1-S_w)\beta_a\rho_a C_a\right]T+(1-n)\rho_s C_s+nS_w\rho_w C_w+n(1-S_w)\rho_a C_a\right\}\dot{T}$$
$$-S_w\rho_w C_w k_w p_{w,i}T_{,i}-S_a\rho_a C_a k_a p_{a,i}T_{,i}-(\lambda_{ij}T_{,j})_{,i}-Q=0 \tag{17}$$

In many situations the temperature and pressure dependence of ρ_π can be neglected for the liquid phase in (16), eliminating several terms in (17).

It has to be reminded that the process under investigation is restricted by the second law of thermodynamics[13]. Equations (5), (14), (15) and (17) describe the coupled heat flow, water flow and airflow in a deforming porous medium. For these equations we have to specify the initial conditions,

$$u_i=u_i^0, \qquad p_\pi=p_\pi^0, \qquad T=T^0 \text{ at } t=0$$

and the boundary conditions,

$$u_i=\bar{u}_i \text{ on } \Gamma_u;\ \sigma_{ij}n_i=t_j \text{ on } \Gamma_t \text{ where } \Gamma_u\cup\Gamma_t=\Gamma$$
$$p_\pi=\bar{p}_\pi \text{ on } \Gamma_{p\pi};\ k_\pi(p_{\pi,i}+\rho_\pi b_i^\pi)n_i-q_\pi=0 \text{ on } \Gamma_{q\pi} \text{ where } \Gamma_{p\pi}\cup\Gamma_{q\pi}=\Gamma$$
$$T=\bar{T} \text{ on } \Gamma_T;$$
$$(S_w\rho_w C_w w_i^w+S_a\rho_a C_a w_i^a)Tn_i-\lambda_{ij}T_{,j}n_i-q_T=0 \text{ on } \Gamma_q \text{ where } \Gamma_T\cup\Gamma_q=\Gamma \tag{18}$$

n_i representing the outward normal of the boundary.

DISCRETIZATION AND SOLUTION

The discretization process is identical to that described in Reference 1. In addition to the variables u_i, p_w, and p_a we have now also T. To obtain the weak form of the energy balance equation we use a Galerkin formulation[12] and terms involving second spatial derivatives are transformed through Gauss' theorem.

Using matrix notation, the discretized equations are,

$$\int_\Omega \mathbf{B}^T\dot{\alpha}''\mathrm{d}\Omega+\mathbf{C}_{sw}\dot{\mathbf{p}}_w+\mathbf{C}_{sa}\dot{\mathbf{p}}_a+\mathbf{C}_{st}\dot{\mathbf{T}}=\dot{\mathbf{f}}_s$$
$$\mathbf{C}_{ws}\dot{\mathbf{u}}+\mathbf{P}_{ww}\dot{\mathbf{p}}_w+\mathbf{C}_{wa}\dot{\mathbf{p}}_a+\mathbf{H}_{ww}\mathbf{p}_w+\mathbf{C}_{wt}\dot{\mathbf{T}}=\dot{\mathbf{f}}_w$$
$$\mathbf{C}_{as}\dot{\mathbf{u}}+\mathbf{C}_{aw}\dot{\mathbf{p}}_w+\mathbf{P}_{aa}\dot{\mathbf{p}}_a+\mathbf{H}_{aa}\mathbf{p}_a+\mathbf{C}_{at}\dot{\mathbf{T}}=\dot{\mathbf{f}}_a$$
$$\mathbf{C}_{tw}\dot{\mathbf{p}}_w+\mathbf{C}_{ta}\dot{\mathbf{p}}_a+\mathbf{P}_{tt}\dot{\mathbf{T}}+\mathbf{H}_{tt}\mathbf{T}=\dot{\mathbf{f}}_t \tag{19}$$

The matrices are listed in the appendix. Equation (19) forms a coupled nonsymmetric and

nonlinear system of ordinary differential equations in time. This can be concisely written as,

$$\mathbf{A}\dot{\mathbf{x}}+\mathbf{C}\mathbf{x}=\dot{\mathbf{F}} \tag{20}$$

where $\mathbf{x}=\{\mathbf{u},\mathbf{p}_w,\mathbf{p}_a,\mathbf{T}\}$ and the matrices **A**, **C**, and **F** are obtained by inspection from (19). For the solution we use the generalized mid-point method which yields the recurrence scheme,

$$(\mathbf{A}+\theta\Delta t\mathbf{C})\mathbf{x}_{n+1}=[\mathbf{A}-(1-\theta)\Delta t\mathbf{C}]\mathbf{x}_n+\Delta t\dot{\mathbf{F}} \qquad 0\leqslant\theta\leqslant 1 \tag{21}$$

The matrices are evaluated at $n+\theta$. Because of the nonlinearities involved a solution scheme of the fixed point type is used within evey time step. In this scheme the first term of the first equation (19) is substituted by the tangent stiffness matrix $\mathbf{K}_T$[17]. As far as the error analysis for the solution is concerned, this can be carried out in the same way as in Reference 1 or, with more detail, in Reference 18.

CONSTITUTIVE EQUATIONS AND TEMPERATURE DEPENDENT PARAMETERS

Soil constitutive models including temperature effects reported in literature are rather limited. Such models can be found, e.g.in References 19–21. The equations of state for water and air, including temperature, are already reported in Reference 1. Other temperature dependent parameters such as the dynamic viscosity of water, relative permeability of water, thermal expansion coefficient and heat capacity of water can be found in Reference 12. Relative permeabilities of air and water are also reported in Reference 22. The relationships between relative permeabilities of water and air, the saturation of water and the capillary pressure proposed Brooks and Corey[23] are used in the numerical simulation. No changes in these relations due to nonisothermal conditions are introduced.

VALIDATION AND APPLICATION EXAMPLES

Firstly the code based on the theory outlined above is validated with respect to fully saturated nonisothermal consolidation. For this purpose a thermoelastic one-dimensional consolidation problem is solved and compared with a previous solution[12]. The same problem is then solved in partially saturated conditions.

A column of linear elastic material is subjected to an external surface load of 1000 N/m^2 and to a surface temperature jump of 50°C above the reference temperature T_{ref} of the column. The boundary conditions are:

- lateral surface $u_h=0$, $q_w=0$, $q_a=0$, $q_T=0$;
- top surface $p_w=p_{atm}$, $p_a=p_{atm}$, $T=T_{ref}+50°C$;
- bottom surface $u_r=0$, $q_w=0$, $q_a=0$, $q_T=0$.

The initial condition for temperature is $T=T_{ref}$ and initial pressures p_w and p_a depend on initial saturation profile as described later. For comparison purposes, the same material properties of the referenced solution[12] are used:

elastic modulus	$E=6000$ kPa
poisson ratio	$\nu=0.4$
permeability	$k=4\times10^{-6}$ m/s
porosity	$n=0.5$
thermal conductivity	$\lambda=0.2$ kCal/m/°C/s
fluid viscosities	$\mu_w=1\times10^{-3}$, $\mu_a=1\times10^{-6}$ Ns/m^2
thermal expansion coefficient	$\beta_s=0.9\times10^{-6}$, $\beta_w=0.63\times10^{-5}$ °C^{-1}
heat capacity	$\rho C=40$ kCal/°C kg
densities	$\rho_s=2000$, $\rho_w=1000$, $\rho_a=1.22$ kg/m^3

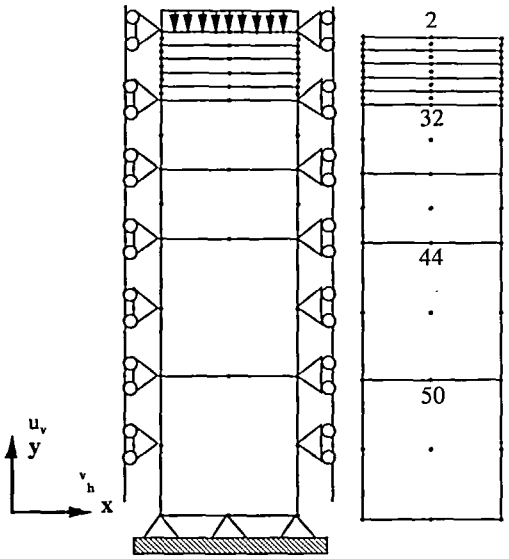

Figure 1 Soil column and finite element spatial discretization

The bulk modulus of water phase and solid phase are 0.43×10^{13} N/m^2 and 0.14×10^{13} N/m^2, respectively, whereas for air the equation of state of a prefect gas is used. The width of the column is 2 metres and the depth 7 metres, as shown in *Figure 1*, where the spatial discretization is also presented.

Temporal discretization is performed with an initial step of 0.01 days and multiplied by 10 after repeating 10 steps until 10^6 days, the required time of analysis.

The problem is solved with three different physical conditions as far as the saturation is concerned: 1) fully saturated, 2) initially homogeneous saturation 0.92, and 3) initial linear distribution from 0.92 at the top surface to 1.0 at the bottom surface. *Figure 2* shows the temperature distribution versus time for different nodes. The distributions are practically the same for the three studied cases where also two different values of the thermal expansion coefficient of water $\beta_w = 0$ and $\beta_w = 0.63 \times 10^{-5}$ °C^{-1} were assumed. This depends on the selected heat capacities and on the saturation distribution which is always high. The same values were obtained as for the fully saturated case in Reference 12 with a different code, as indicated in *Figure 2*. In *Figure 3* vertical displacements for selected points are presented for cases 1) and 2). The effect of partial saturation upon the reduction of the consolidation phase is remarkable at onset of the phenomenon, whereas the swelling effect due to temperature is considerable at high time values for both cases. *Figure 4* depicts the temperature effects on vertical displacements at different points within the column in case 3). For comparison reasons also the isothermal solution is shown, as well as an isothermal solution obtained with a different code under static air phase assumption, i.e. the air phase remains at atmospheric pressure. In this example the swelling of the sample is only due to temperature effects. *Figure 5* shows the comparison of saturation histories with isothermal and nonisothermal effects.

As a next example, the problem solved by Dakshanamurthy and Fredlund[4] is solved. The model applied by the two above authors was shortly discussed in the introduction. The problem is that of moisture and heat flow in an unsaturated subgrade soil below a highway or airfield pavement due to the effect of environmental change. The subgrade system is assumed initially in a state of equilibrium. Then sudden environmental changes are imposed at the boundary,

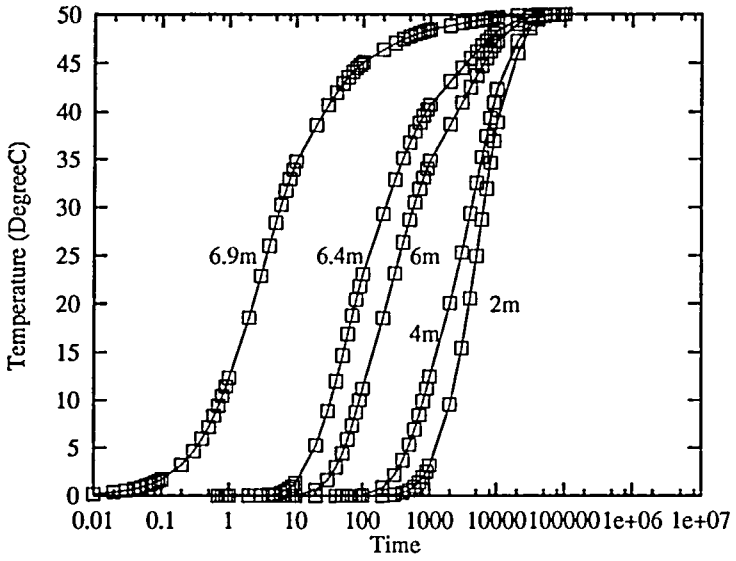

Figure 2 Temperature variation versus time at different nodes, squares indicate solution from Lewis and Schrefler[12]

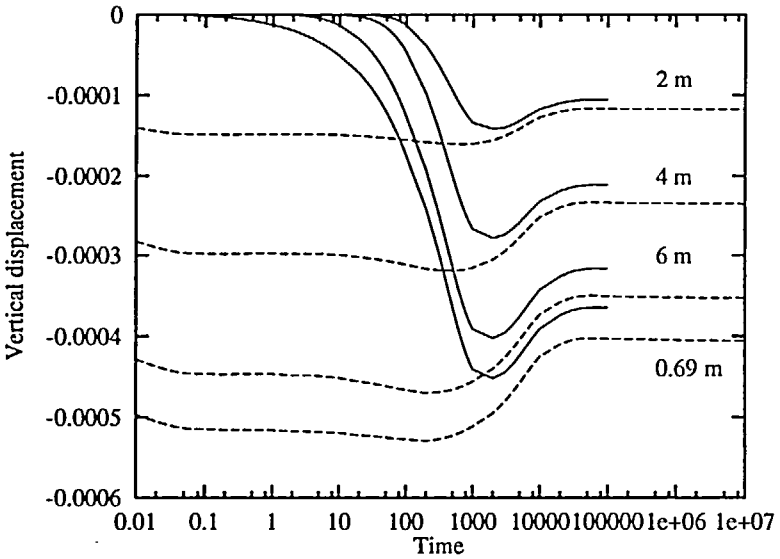

Figure 3 Comparison between saturated (solid line) and unsaturated, $S_w = 0.92$, (dotted line) solution

where evaporation or infiltration builds up an excess pore water pressure, respectively positive or negative with respect to the equilibrium state. This overpressure and temperature gradient cause simultaneous flow of water and air. In the present fully coupled simulation, the same constitutive relationships are used both for the infiltration (wetting) and evaporation (drying) case. Hysteresis effects are hence disregarded. Obviously the computer code can handle different relationships, even though the presence of wetting and drying in the same simulation results in further difficulties for the numerical analysis. Again the soil deformation is taken into account.

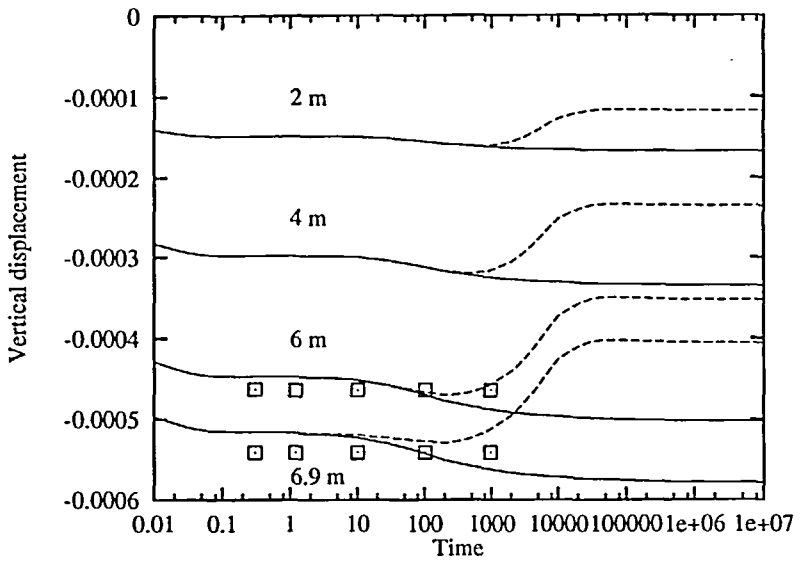

Figure 4 Comparison between nonisothermal (dotted line) and isothermal (solid line), squares indicate solution for isothermal case and static air phase assumption for unsaturated case 3

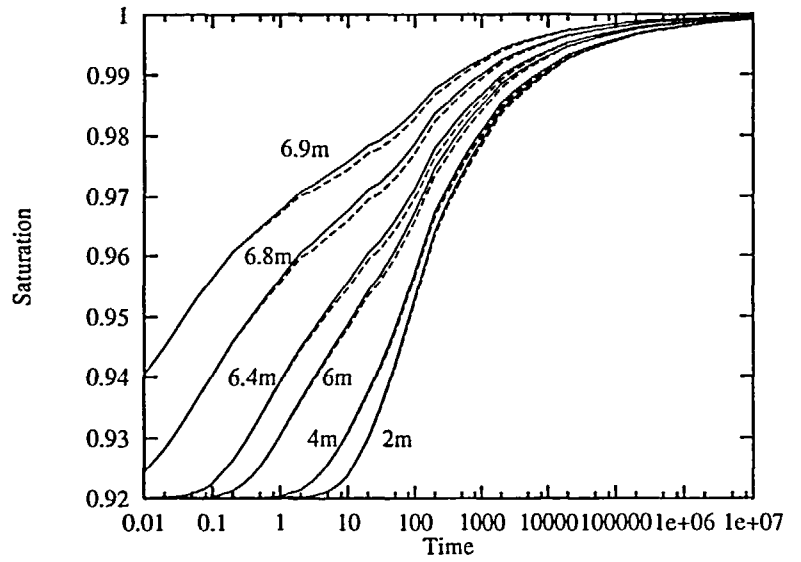

Figure 5 Resulting saturation versus time for nonisothermal (dotted line) and isothermal (solid line) analysis for case 3

The initial conditions are: $T = 10°C$, $p_a = 102\,000\ N/m^2$, $p_w = -420\,000\ N/m^2$ for infiltration case and $p_w = -280\,000\ N/m^2$ for evaporation case respectively.

The boundary conditions are:

- lateral surface $u_h = 0$, $q_w = 0$, $q_a = 0$, $q_T = 0$;
- top surface $T = 25°C$, $p_a = 102\,000\ N/m^2$, $p_w = -280\,000\ N/m^2$ for infiltration case and $p_w = -420\,000\ N/m^2$ for evaporation case respectively;
- bottom surface $u_v = 0$, $q_w = 0$, $q_a = 0$, $q_T = 0$.

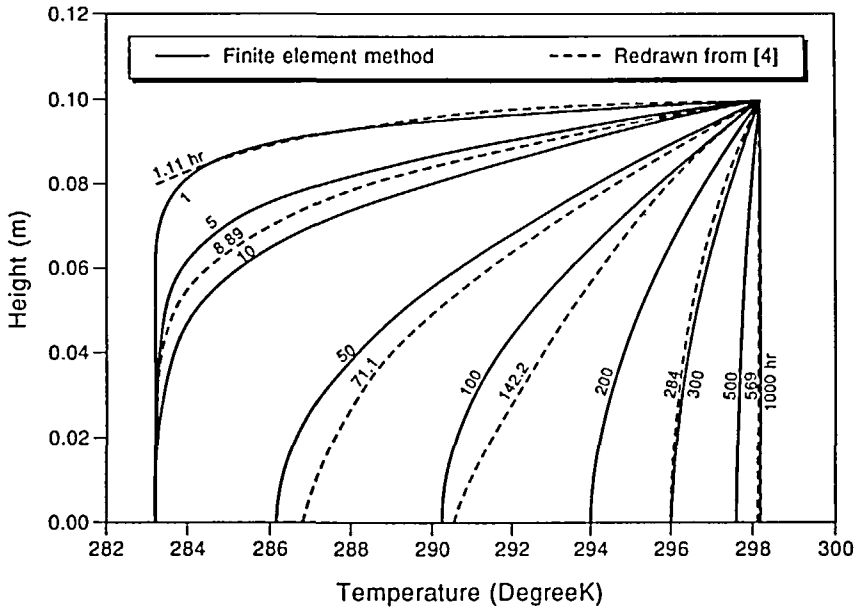

Figure 6 Profile of the temperature during consolidation. Dotted lines are redrawn from Dakshanamurthy and Fredlund[4]

Time step is initially one hour and then increased by one order after ten steps until 1000 hours.

In the following figures, where possible, our results are compared with those of Reference 4. *Figure 6* shows the comparison of the temperature within the clay layer as a result of an increase in the temperature from 10°C (283.2°K) to 25°C (298.2°K) under evaporation condition. The figure illustrates how the imposed thermal increase at the surface is slowly transferred to the bottom of soil and equilibrium with the new boundary condition is eventually reached. The same diagram is obtained also for the temperature increase under infiltration conditions. The different behaviour of our model when compared with Reference 4 is mainly due to the temperature and pressure dependence of the air density through the state equation of a prefect gas. *Figure 7* depicts the comparison of the pore water pressure distribution throughout the clay layer due to a change in the pore water pressure at the top surface. The pore water pressure was initially −280 kPa, and then changed to a value of −420 kPa instantaneously, assumed due to evaporation. Here the difference in time transient behaviour is enhanced due to the difference in the models. *Figure 8* shows the corresponding pore air pressure distributions throughout the clay layer under volume decrease or consolidation process and *Figure 9* presents the distribution of saturation throughout the clay layer, under the consolidation process which is shown in *Figure 10*. The following Figures depict the reverse processes, i.e. infiltration conditions are here considered together with the same temperature increase as in *Figure 6*. *Figure 11* depicts the comparison of the pore water pressure distribution in the clay layer. Recalling that the pore water pressure was initially −420 kPa, and then suddenly changed at the boundary to a value of −280 kPa to simulate infiltration. *Figure 12* presents the distribution of saturation throughout the clay layer, under the swelling process. From the different behaviour of the compared models it appears important to take into account temperature and pressure dependence of the fluid parameters as well as airflow due to temperature gradients.

To assess the effect of the deformability of the solid skeleton on the other involved fields, a further numerical simulation was performed using the same parameters are above, except for

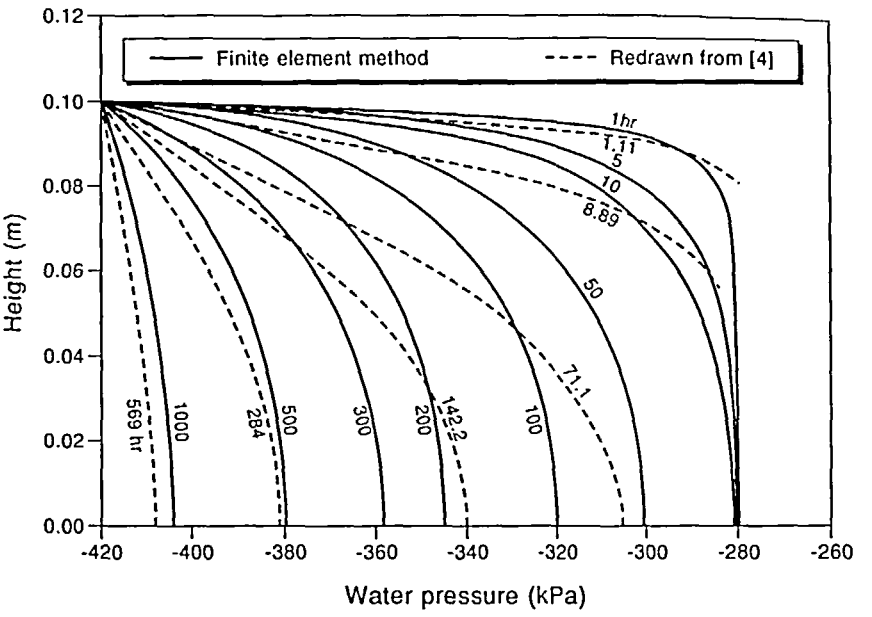

Figure 7 Profile of the water pressure during consolidation. Dotted lines are redrawn from Dakshanamurthy and Fredlund[4]

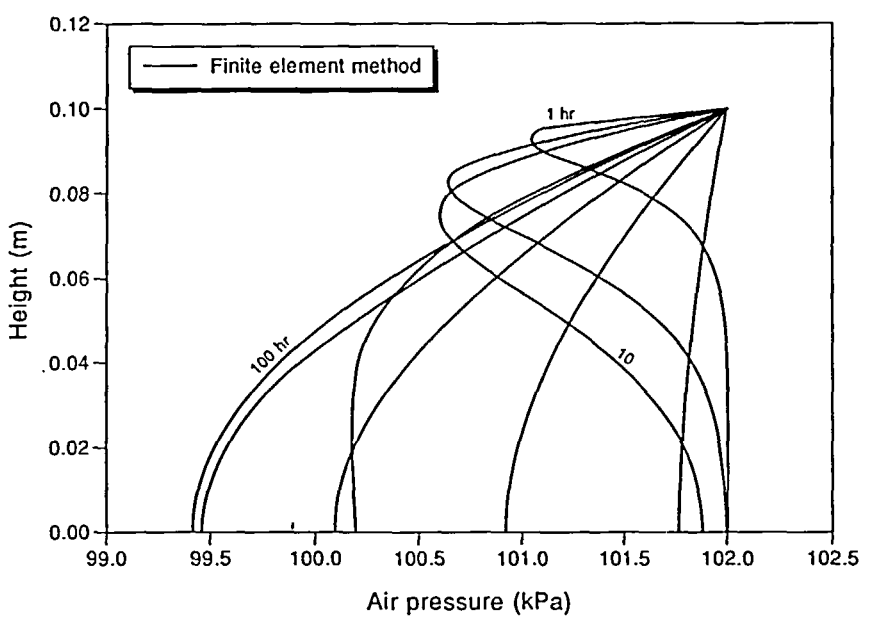

Figure 8 Profile of the air pressure during consolidation

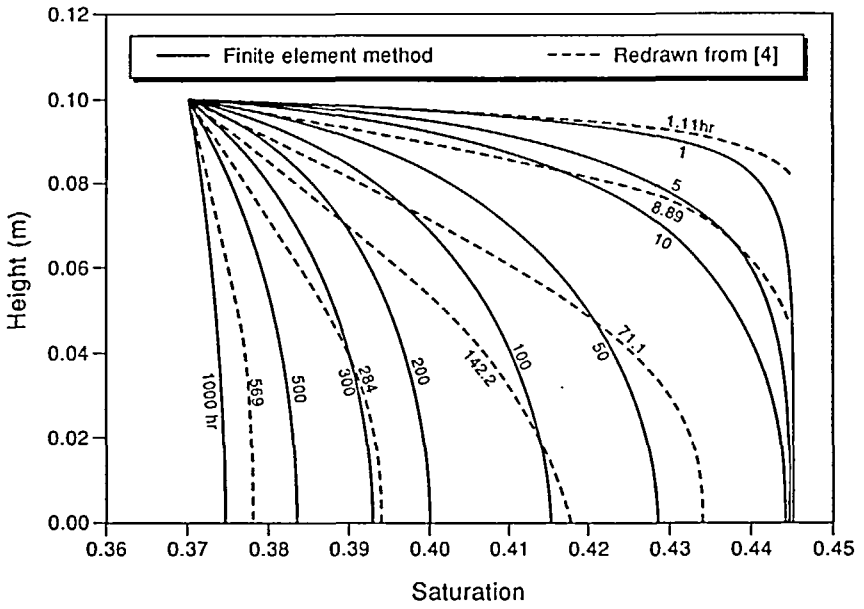

Figure 9 Profile of the saturation during consolidation. Dotted lines are redrawn from Dakshanamurthy and Fredlund[4]

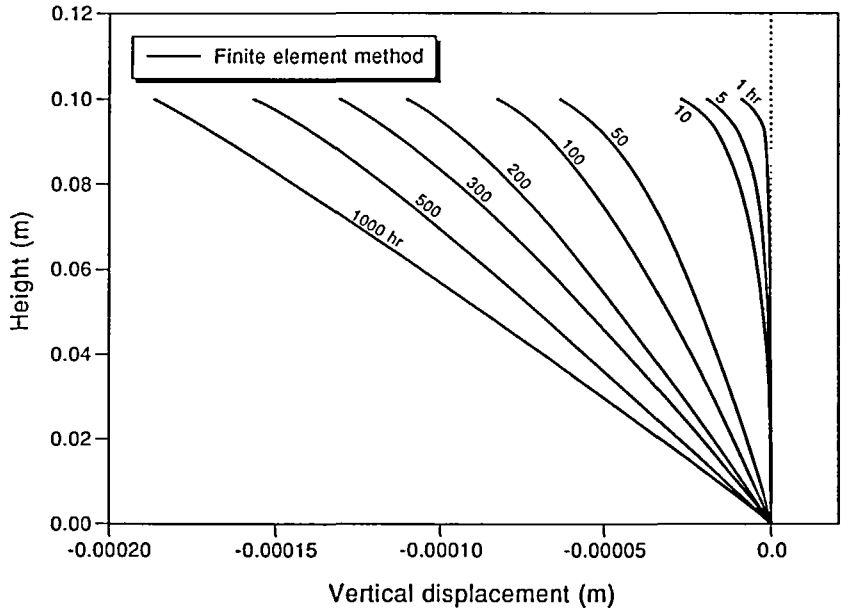

Figure 10 Profile of the vertical displacement during consolidation

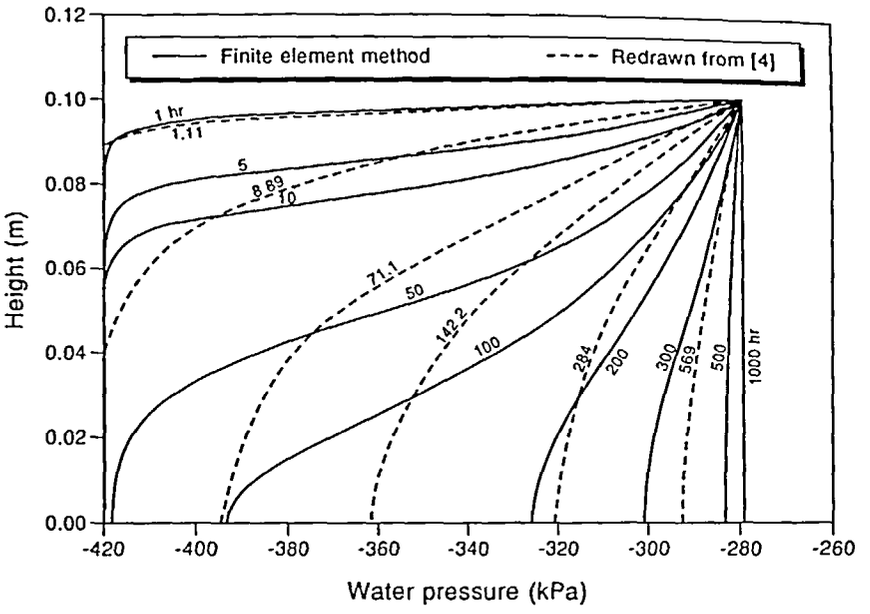

Figure 11 Profile of the water pressure during swelling. Dotted lines are redrawn from Dakshanamurthy and Fredlund[4]

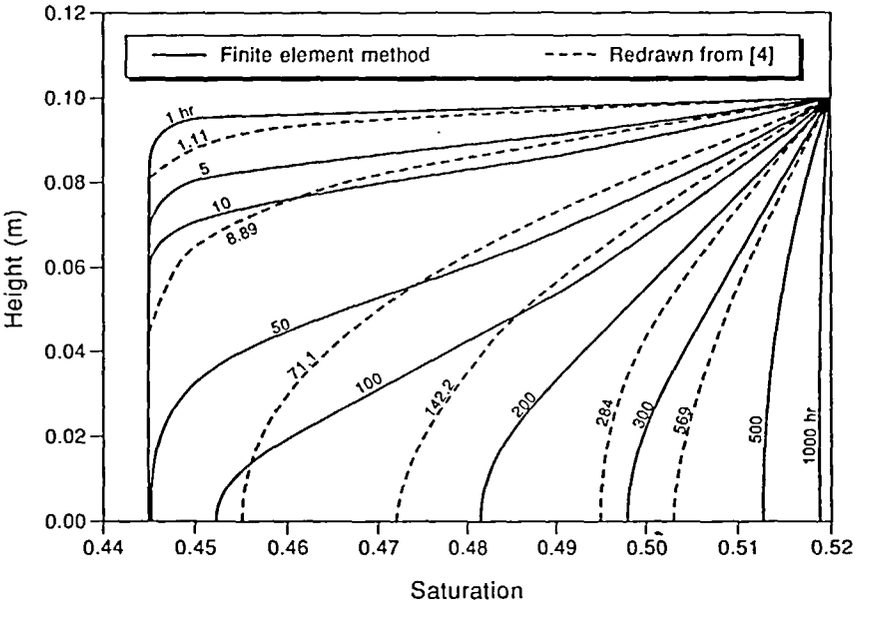

Figure 12 Profile of the saturation during swelling. Dotted lines are redrawn from Dakshanamurthy and Fredlund[4]

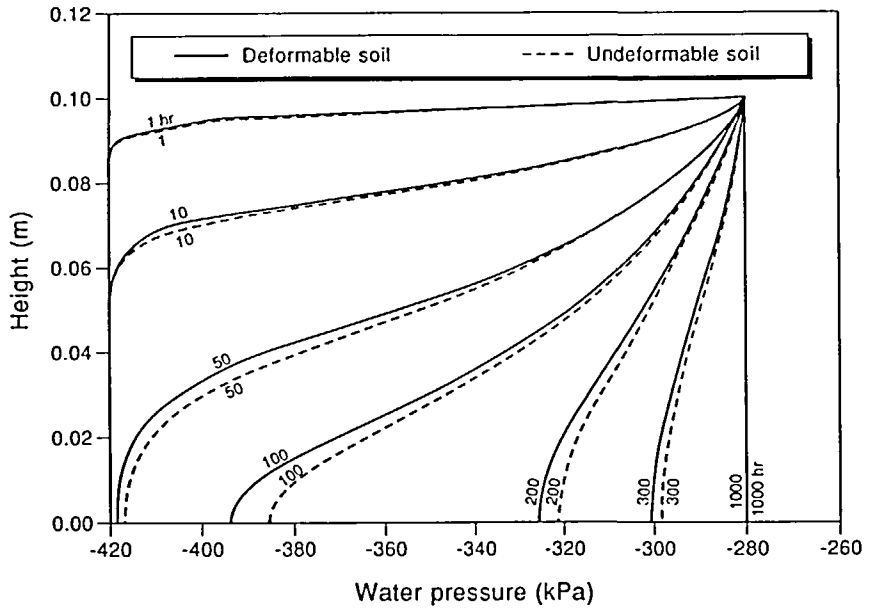

Figure 13 Profiles of water pressure during swelling for a deformable (solid lines) and a very stiff soil (dotted lines)

the soil Young's modulus, which was assumed 100 times larger. *Figure 13* shows the obtained results in terms of water pressure for the swelling case. This influence is evident, mainly at intermediate times of the analysis and results in a slower dissipation of the pressure change when deformable soil is considered.

CONCLUSIONS

A fully coupled model for simulating the complex behaviour of multiphase fluid and heat flow in deformable porous media has been presented. The model consists of a group of nonlinear and coupled partial difference equations, namely, (1) the equilibrium equation for soil; (2) the continuity equations for aqueous and non-aqueous phase fluids; (3) the energy conservation equation. These equations are solved by the finite element methods and soil displacements, aqueous and non-aqueous phase fluid pressure, and temperature are the unknown variables. Several thermal effects are taken into account such as flow due to temperature gradients, temperature dependent soil parameters and capillary pressure relationship and heat transfer through conduction and convection. The validity of the approach hs been demonstrated by two examples. Further developments of this model will include also latent heat transfer which becomes important when the temperature gradients are no longer small.

APPENDIX

The matrices in the discretized equations (19) are shown here in detail, using the notation of Reference 12.

$$\mathbf{K}_T = -\int_\Omega \mathbf{B}^T \mathbf{D}_T \mathbf{B} \mathrm{d}\Omega$$

$$\mathbf{C}_{sw} = \int_\Omega \mathbf{B}^T \alpha \mathbf{m} \left[S_w + (p_a - p_w) \frac{\partial S_w}{\partial p_c} \right] \mathbf{N} \mathrm{d}\Omega$$

$$\mathbf{C}_{sa} = \int_\Omega \mathbf{B}^T \alpha \mathbf{m} \left[S_a - (p_a - p_w) \frac{\partial S_w}{\partial p_c} \right] \mathbf{N} \mathrm{d}\Omega$$

$$\mathbf{C}_{st} = \int_\Omega \mathbf{B}^T \left[\mathbf{D}_T \mathbf{m} \frac{\beta_s}{3} - \alpha (p_a - p_w) \frac{\partial S_w}{\partial T} \mathbf{m} \right] \mathbf{N} \mathrm{d}\Omega$$

$$\dot{\mathbf{f}}_s = \int_\Omega \mathbf{N}^T \frac{\mathrm{d}\mathbf{b}}{\mathrm{d}t} \mathrm{d}\Omega + \int_\Gamma \mathbf{N}^T \frac{\mathrm{d}\mathbf{t}}{\mathrm{d}t} \mathrm{d}\Gamma$$

$$\mathbf{C}_{ws} = \int_\Omega \mathbf{N}^T S_w \mathbf{m}^T \alpha \mathbf{B} \mathrm{d}\Omega$$

$$\mathbf{P}_{ww} = \int_\Omega \mathbf{N}^T \left\{ -n \frac{\partial S_w}{\partial p_c} + \frac{n S_w}{K_w} + S_w \frac{\alpha - n}{K_s} \left[S_w + (p_a - p_w) \frac{\partial D_w}{\partial p_c} \right] \right\} \mathbf{N} \mathrm{d}\Omega$$

$$\mathbf{C}_{wa} = \int_\Omega \mathbf{N}^T \left\{ n \frac{\partial S_w}{\partial p_c} + S_w \frac{\alpha - n}{K_s} \left[S_a - (p_a - p_w) \frac{\partial S_w}{\partial p_c} \right] \right\} \mathbf{N} \mathrm{d}\Omega$$

$$\mathbf{H}_{ww} = \int_\Omega (\nabla \mathbf{N})^T \mathbf{k}_w \nabla \mathbf{N} \mathrm{d}\Omega$$

$$\mathbf{C}_{wt} = \int_\Omega \mathbf{N}^T \left\{ \left[n - \frac{(\alpha - n) S_w}{K_s} (p_a - p_w) \right] \frac{\partial S_w}{\mathrm{d}T} - [n\beta_w + (\alpha - n)\beta_s] S_w \right\} \mathbf{N} \mathrm{d}\Omega$$

$$\dot{\mathbf{f}}_w = -\int_\Omega (\nabla \mathbf{N})^T \mathbf{k}_w \nabla (\rho_w b_w) \mathrm{d}\Omega - \int_\Gamma \mathbf{N}^T q_w \mathrm{d}\Gamma$$

$$\mathbf{C}_{as} = \int_\Omega \mathbf{N}^T S_a \mathbf{m}^T \alpha \mathbf{B} \mathrm{d}\Omega$$

$$\mathbf{C}_{aw} = \int_\Omega \mathbf{N}^T \left\{ n \frac{\partial S_w}{\partial p_c} + S_a \frac{\alpha - n}{K_s} \left[S_w + (p_a - p_w) \frac{\partial S_w}{\partial p_c} \right] \right\} \mathbf{N} \mathrm{d}\Omega$$

$$\mathbf{P}_{aa} = \int_\Omega \mathbf{N}^T \left\{ -n \frac{\partial S_w}{\partial p_c} + \frac{n S_a}{K_a} + S_a \frac{\alpha - n}{K_s} \left[S_a - (p_a - p_w) \frac{\partial S_w}{\partial p_c} \right] \right\} \mathbf{N} \mathrm{d}\Omega$$

$$\mathbf{H}_{aa} = \int_\Omega (\nabla \mathbf{N})^T \mathbf{k}_a \nabla \mathbf{N} \mathrm{d}\Omega$$

$$\mathbf{C}_{at} = \int_\Omega \mathbf{N}^T \left\{ \left[n + \frac{(\alpha - n) S_a}{K_s} (p_a - p_w) \right] \frac{\partial S_w}{\partial T} - [n\beta_a + (\alpha - n)\beta_s] S_a \right\} \mathbf{N} \mathrm{d}\Omega$$

$$\dot{\mathbf{f}}_a = -\int_\Omega (\nabla \mathbf{N})^T \mathbf{k}_a \nabla (\rho_a b_a) \mathrm{d}\Omega - \int_\Gamma \mathbf{N}^T q_a \mathrm{d}\Gamma$$

$$\mathbf{C}_{tw}=\int_\Omega \mathbf{N}^T\left[\frac{(1-n)\rho_s C_s}{K_s}\left(S_w+(p_a-p_w)\frac{\partial S_w}{\partial p_c}\right)-n\rho_w C_w\frac{\partial S_w}{\partial p_c}+\frac{nS_w\rho_w C_w}{K_w}+n\rho_a C_a\frac{\partial S_w}{\partial p_c}\right]T\mathbf{N}\mathrm{d}\Omega$$

$$\mathbf{C}_{ta}=\int_\Omega \mathbf{N}^T\left[\frac{(1-n)\rho_s C_s}{K_s}\left(S_a-(p_a-p_w)\frac{\partial S_w}{\partial p_c}\right)+n\rho_w C_w\frac{\partial S_w}{\partial p_c}+\frac{nS_a\rho_a C_a}{K_a}-n\rho_a C_a\frac{\partial S_w}{\partial p_c}\right]T\mathbf{N}\mathrm{d}\Omega$$

$$\mathbf{P}_{tt}=\int_\Omega \mathbf{N}^T\left\{\left[\frac{(n-1)\rho_s C_s'}{K_s}(p_a-p_w)\frac{\partial S_w}{\partial T}+(n-1)\beta_s\rho_s C_s+n\rho_w C_w\frac{\partial S_w}{\partial T}-nS_w\beta_w\rho_w C_w\right.\right.$$
$$\left.\left.-n\rho_a C_a\frac{\partial S_w}{\partial T}-n(1-S_w)\beta_a\rho_a C_a\right]T+(1-n)\rho_s C_s+nS_w\rho_w C_w+n(1-S_w)\rho_a C_a\right\}\mathbf{N}\mathrm{d}\Omega$$

$$\mathbf{H}_{tt}=\int_\Omega \mathbf{N}^T(S_w\rho_w C_w k_w p_{w,i}+S_a\rho_a C_a k_a p_{a,i})\nabla\mathbf{N}\mathrm{d}\Omega+\int_\Omega(\nabla\mathbf{N})^T\lambda_{ij}\nabla\mathbf{N}\mathrm{d}\Omega$$

$$\dot{\mathbf{f}}_t\int_\Omega \mathbf{N}[(1-n)\rho_s Q_s+n\rho_w S_w Q_w+n\rho_a S_a Q_a]\mathrm{d}\Omega-\int_\Gamma \mathbf{N}q_T\mathrm{d}\Gamma$$

ACKNOWLEDGEMENTS

This research was partially supported by the Italian Ministry of University and Scientific and Technological Research (Grant MURST 40%).

REFERENCES

1 Schrefler, B. A. and Zhan Xiaoyong. A fully coupled model for water flow and airflow in deformable porous media, *Water Resour. Res.*, **29** (1), 155–167 (1993)
2 Philip, J. R. and de Vries, D. A. Moisture movement in porous materials under temperature gradients, *Trans. Amer. Geopys. Union*, **38**, 222–232 (1957)
3 Alonso, E. E., Gens, A. and Hight, D. W. Special problem soils: General report, *Proc. 9th European Conf. on Soil Mechanics and Foundation Eng.*, **3**, 1087–1146, Bakema, Rotterdam (1987)
4 Dakshanamurthy, V. and Fredlund, D. G. A mathematical model for predicting moisture flow in an unsaturated soil under hydraulic and temperature gradients, *Water Resour. Res.*, **17**, 714–722 (1981)
5 Thomas, H. Modelling two-dimenisonal heat and moisture transfer in unsaturated soils, including gravity effects, *Int. J. Numer. Anal. Methods Geomech.*, **9**, 573–588 (1985)
6 Luikov, A. V. Heat and Mass Transfer in Capillary Porous Bodies, Pergamon Press, Oxford (1966)
7 Thomas, H. R. and King, S. D. Coupled temperature/capillary potential variation in unsaturated soils, *J. Eng. Mech.*, **117** (11), 2475–2490 (1991)
8 Baggio, P., Majorana, C. E. and Schrefler, B. A. Hydrothermomechanical analysis of concrete by a finite element method, *Proc. of the 8th Int. Conf. on Num. Meth. for Thermal Problems*, R. W. Lewis, ed., Pineridge Press, Swansea, 847–859 (1993)
9 Geraminegad, M. and Saxena, S. K. A coupled thermoelastic model for saturated-unsaturated porous media, *Geotechnique*, **36** (4), 539–550 (1986)
10 Lewis, R. W., Roberts, P. J. and Schrefler, B. A. Finite element modelling of two phase heat and fluid flow in deforming porous media, *J. Transport Porous Media*, **4**, 319–334 (1989)
11 Schrefler, B. A., Simoni, L., Li, X. and Zienkiewicz, O. C. Mechanics of partially saturated porous media, *Num. Meth. and Constitutive Modelling in Geomechanics*, CISM Courses and Lectures, **311**, ed. Desai, C. S. and Gioda, G. 169–209, Springer-Verlag (1990)
12 Lewis, R. W. and Schrefler, B. A. *The Finite Element Method in the Deformation and Consolidation of Porous Media*, John Wiley, New York (1987)
13 Coussy, O. *Mecanique des Milieux Poreux, Editions Technip*, Paris, 1991
14 de Boer, R., Ehlers, W., Kowalski, S. and Plischka, J. *Porous media, a survey of different approaches*, Fachbereich Bauwesen der Universitat Gesamthochschule-Essen, Heft 54 (1991)
15 Bear, J. and Bachmat, Y. *Introduction to modeling of transport phenomena in porous media*, Kluwer Academic Pub., Dordrecht (1991)

16 Schrefler, B. A., Simoni, L. and Baggio, P. Heat and mass transfer in deformable porous media, in *Finite Elements in Fluids*, 846–855, Morgan, K., Oñate, E., Periaux, J., Peraire, J. and Zienkiewicz, O. C. (Eds.), CIMNE/Pineridge (1993)
17 Schrefler, B. A., Simoni, L., Turska, E. and Zhan, X. Y. Zur Berechnung von ungesättigten Konsolidationsproblemen, *Bauingenieur*, **9**, 375–384 (1993)
18 Turska, E. and Schrefler, B. A. On convergence conditions of partitioned solution procedures for consolidation problems, *Comp. Meth. in Applied Mech. and Eng.*, **106**, 51–63 (1993)
19 Desai, C. S. and Zhang, D. Viscoplastic model for geologic materials with generalized flow rule, *Int. J. Numer. Anal. Meth. Geomech.*, **11**, 603–620 (1987)
20 Hueckel, T. and Pellegrini, R. Thermoplastic modelling of undrained failure of saturated clay due to shearing, *Soils and Foundations*, **31** (3), 1–16 (1991)
21 Laloui, L. *Modelisation du comportement thermo-hydro-mecanique des milieux poreaux anelastiques*, These de docteur-ingenieur of Ecole Centrale de Paris, 92295 Chatenay Malabry (1993)
22 Scheidegger, A. E. *The Physics of Flow through Porous Media*, University of Toronto Press, Toronto (1974)
23 Brooks, R. N. and Corey, A. T. Properties of porous media affecting fluid flow, *J. Irrig. Drain. Div. Am. Soc. Civ. Eng.*, **92**(IR2), 61–68 (1966)